

## Testing singularities in the complex plane: Suggestions for dendritic-growth experiments

Martine Ben Amar and Efim Brener\*

*Laboratoire de Physique Statistique, Ecole Normale Supérieure, 24 rue Lhomond, 75231 Paris 5, France*

(Received 8 June 1992)

The usual theories of selection in dendritic growth involve an analytical extension in the complex plane and a search of singularities for the profile function. We show here that the complex plane is in fact the liquid phase and that the zone of singularity lies on the growth axis. We find a selection mechanism, by using localized perturbations, for the dendritic growth even when the surface tension is isotropic. We show that it is possible to act on the complex plane and to modify at distances the growth rate and the shape of the solidification front. Moreover, we stress here the influence of localized perturbations on the measurement of the constant of stability  $\sigma^*$  of the needle crystal.

PACS number(s): 68.70.+w, 61.50.Cj, 05.70.-a, 81.30.Fb

### I. INTRODUCTION

During the past two decades, physicists have tried to understand the selection mechanism for observed needle crystals. It has long been known that solidification of a crystal results in dendrites and only the product of the tip radius times the growth rate is fixed by the undercooling [1]. A series of numerical and analytical papers (for reviews, see [2]) based on the solution of the steady-state growth equations conclude that suitable solutions can exist if and only if one introduces explicitly the anisotropy of surface tension. They predict that the “constant of stability”  $\sigma^* = 2d_0D/\rho^2U$  (with  $d_0$  the capillary length,  $D$  the diffusion coefficient,  $\rho$  the tip radius, and  $U$  the growth rate) depends only on  $\epsilon$ , the anisotropy coefficient, with an  $\epsilon^{7/4}$  [3] dependence for small  $\epsilon$ . Very unfortunately, to date, this coefficient has been reported only for five materials and the discrepancy between calculated and measured  $\sigma$  values remains of order two or three, in both directions [4]. This is a little disconcerting after several decades of hard work.

Moreover, as far as the selection mechanism is concerned, such a discrepancy between measured characteristic lengths and predicted ones does not exist for viscous fingering, even in the very unstable radial geometry [5]. The parallelism between the equations which govern both instabilities is perfectly well established, even if the conformal-mapping techniques [6] are generally preferred for Laplacian growth. Nevertheless, the selection treatment is the same: analytical continuation of the interface equation in the complex plane and search of singularities in this plane. Of course, this similarity does not help one very much to understand what happens really in crystal growth. But one can notice that it would be very pleasant to have an adjustable parameter in dendritic growth, completely in the hand of the experimentalist, instead of the parameter  $\epsilon$ , which is imperfectly known. In viscous fingering, this is the case, since the capillary number  $\sigma$  depends on the pushing flux and can be varied continuously by the experimentalist.

Our attention has been drawn by the paper by Thomé *et al.* [7], whose very suggestive title is “Controlling

singularities in the complex plane: Experiments in real space.” The aim of that paper, which concerns viscous fingering in a channel, was to show that the complex plane of the theoreticians is in fact the liquid viscous fluid, so that it is possible to act on it. They obtain fingers in the forbidden range of  $\lambda$  values ( $\lambda$  is the half width of the finger compared to the channel width,  $\lambda > 0.5$ ). To do so, they create a singularity of the fluid velocity by putting a coin in front of the finger, on the growth axis. This new but physical singularity competes with the unique singularity induced by curvature in the range  $\lambda < 0.5$ , so narrow fingers are permitted. In the limit of a very low capillary number and weak perturbation, a collapse condition is enough to fix  $\lambda$ , which depends only on the position of the coin in front of the tip, on the growth axis. Is it possible to adapt this result to the needle crystal growth? This is one purpose of the present paper.

First of all, we consider the crystal-growth regime which is formally the closest to viscous fingering: the one-sided model of solidification at low Péclet number. We show that the singular point due to curvature is located on the growth axis, in front of the tip at a distance of 1.5 times the tip radius of the dendrite. So conceptually the situation appears to be very similar to viscous fingering. As a consequence, in the absence of anisotropy of surface tension, a needle crystal exists if one adds a static and localized perturbation in front of the crystal. As a perturbation, one can think of an obstacle, of a germ or an inhomogeneity of temperature or impurity. We analyze these perturbations and show that they are equivalent to a dipole for the impurity or temperature field. But due to the lack of intrinsic length scale in the dendritic growth problem, the amplitude of the perturbation itself is dependent on the unknown radius of curvature. This complicates the analysis and requires a numerical study. When anisotropy is added, we show that a dipole perturbation on the growth axis located at a distance of the order of the tip radius increases very significantly the constant of stability  $\sigma^*$ . Since we show that most of the physical perturbations encountered in experiments are equivalent to fictitious dipoles, one can easily imagine

that it is very difficult to measure this constant of stability  $\sigma^*$  with precision, and to test the theory of selection, which has been established in a too ideal situation.

This paper is organized as follows. In Sec. II, we show that we can also treat the dendritic growth at low Péclet numbers by conformal-mapping techniques stressing the similarity between growth, viscous fingering, and usual electrostatics. Section III recovers known results about the selection problem within this framework. Section IV gives a simplified description of localized perturbations in terms of dipoles. Section V shows that these perturbations can also be responsible of the selection process. Finally, in Sec. VI we confirm numerically our analytical predictions and study the competition between the anisotropy of surface tension  $\epsilon$  and a dipolar perturbation, both in the two-dimensional (2D) and 3D cases.

## II. THE ZERO-SURFACE TENSION FREE-BOUNDARY PROBLEM

In this section, we consider the steady growth of a needle crystal in the one-sided model of solidification, in two dimensions. This model represents fairly well the solidification induced by diffusion of impurities, but our conclusions, as shown below by the numerics, are also valid for the symmetric model of solidification (more convenient for thermal processes) in two or three dimensions with axisymmetry. Moreover, we restrict ourselves to vanishing Péclet numbers (the Péclet number is a dimensionless quantity defined by the characteristic length of the growing structure times the growth velocity  $U$  divided by the diffusion coefficient  $D_c$ ). We will deal with the Laplace equation in the liquid phase rather than the diffusion equation for different reasons. First, our analysis will be similar to the one employed for the Saffman-Taylor viscous fingering, the main differences coming from boundary conditions at the walls and at infinity. Second, we will take advantage of simple results of electrostatics to justify the selection mechanism with or without localized perturbation. It is certain that some results derived in this paper have been known for several years now, but they have been obtained by a rather sophisticated analysis of nonlinear integral equations. Our purpose is also to find a more pedagogical way to derive the so-called “selection mechanism.”

Exact results are more easily derived for Laplacian fields, because we can use conformal-mapping techniques which rest on the existence of a complex potential. In this part, we want to recover the exact results of Ivantsov [1] by this technique, in order to handle the free-boundary problem with both capillarity and localized perturbations as has been done for the Saffman-Taylor problem [7,8]. As for the usual Laplacian field, we map the physics  $(x,y)$  plane to the complex potential one  $\Phi=(\phi,\psi)$ .  $\phi$  has an obvious physical meaning: it represents the dimensionless concentration field  $\phi=(c-c_L)/(c_L-c_S)$ ;  $c$  is the impurity concentration in the liquid phase and  $c_L$  ( $c_S$ ) is given by the liquidus (solidus) lines of the phase diagram. In a hydrodynamic experiment  $\psi$  is the stream function. In our case, its physical meaning is less obvious but we can define it, at

least mathematically. The diffusion length given by  $D_c/U$  (for a discussion of scaling laws, see, for example, [9]) is large when  $\Delta$ , the supersaturation at infinity, is small. So we can surely use the Laplace approximation around the tip of the needle crystal as soon as one considers distances of order of the tip radius. It gives

$$\Delta\phi(x,y)=0+O(\text{Pe}) \quad \text{with } \text{Pe}=\frac{2\rho U}{D_c}. \quad (2.1)$$

So  $\phi$  can be considered as the real part of an analytical function (see Fig. 1, which represents the frame coordinates). The imaginary part  $\psi$  can be derived by solving the Cauchy equations, as soon as  $\phi$  is known everywhere. This equation (2.1) must be solved simultaneously with boundary conditions at the interface: the Stefan law and the Gibbs-Thomson law. The Stefan law gives the flux of impurity across the interface,

$$\mathbf{n}\cdot\nabla\phi=-\frac{\partial\Psi}{\partial s}=-\text{Pe}\cos\theta, \quad (2.2)$$

while the Gibbs-Thomson law fixes the impurity amount at the interface,

$$\phi|_{\Gamma}=\frac{d_0}{2\rho}\frac{\partial\theta}{\partial s}. \quad (2.3)$$

We take as the length unit two times the tip radius of curvature of the Ivantsov parabola,  $\theta$  is the angle between the growth direction and the normal  $\mathbf{n}$  of the interface, and  $s$  is the dimensionless arclength.  $d_0$  is the capillary length, which is taken equal to zero in this section.  $\Gamma$  is the interface. It will be more convenient to transform (2.2) into

$$\left.\frac{\partial y}{\partial\phi}\right|_{\Gamma}=-\frac{1}{\text{Pe}}. \quad (2.4)$$

The reader may think that the present model and especially Eqs. (2.1) and (2.2) are inconsistent since we do not keep the same order in  $\text{Pe}$  in both equations. For a complete discussion of this question, we refer to the paper by

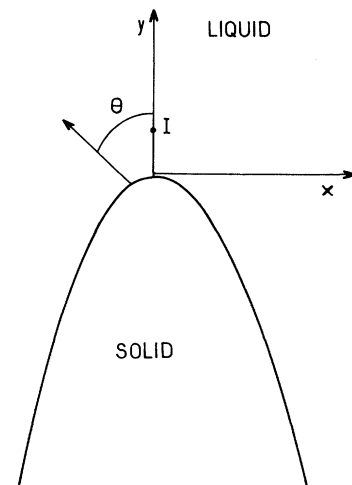


FIG. 1. The needle-crystal frame of coordinates.

Pelcé and Pomeau, who justify this approach via an asymptotic analysis [10]. To guess a complex potential with parabolic isoconcentration lines is not very difficult. In fact, the solution is given explicitly in the lectures of Feynman [11]:

$$iz = -\frac{1}{\text{Pe}^2} \left[ \phi - \frac{\text{Pe}}{2} + i\psi \right]^2 + \frac{1}{4}. \quad (2.5)$$

The interface is deduced from the Gibbs-Thomson law in the absence of capillary effects ( $\phi=0$ ), which gives

$$x = \frac{\psi}{\text{Pe}}, \quad y = -\left[ \frac{\psi}{\text{Pe}} \right]^2 \quad \text{so } y = -x^2. \quad (2.6)$$

With this choice [Eq. (2.5)], the reader can check that the Stefan law (2.4) is automatically satisfied and, as in the Ivantsov theory, the lines of isoconcentration are parabolas of equation:

$$y = \left[ \left[ \frac{\phi}{\text{Pe}} \right]^2 - \frac{\phi}{\text{Pe}} - x^2 / \left[ \frac{2\phi}{\text{Pe}} - 2 \right]^2 \right].$$

This result is consistent with the Ivantsov treatment, when  $\Delta$ , the supersaturation at infinity, goes to zero. Nevertheless, it gives no way to derive explicitly the relation between the Péclet number and  $\Delta$ , which is reached for values of  $\phi$  of order  $\text{Pe}^{1/2}$ . This restricts its validity to  $\phi$  values of order  $\text{Pe}^{1/2}$  or less. Fortunately, it turns out that the selection mechanism results from interactions which act on distances of order of the tip radius, which means  $\phi$  of order  $\text{Pe}$ , as shown in the next section.

### III. FREE-BOUNDARY PROBLEM WITH CAPILLARITY

We want to show here that this formalism allows one to treat rather easily the selection mechanism by surface tension of the 2D needle crystal. Let us first introduce a function of the unknown profile:  $f = e^{i\theta}$  ( $\theta$  has been defined above). For an arbitrary point of the interface  $\Gamma$ , the two boundary conditions to apply to the interface can be joined together into a unique equation concerning the complex derivative of the complex potential:

$$\begin{aligned} \frac{d\Phi}{dz} \Big|_{\Gamma} &= \frac{1}{f} \left[ \frac{\partial\phi}{\partial s} + i \frac{\partial\psi}{\partial s} \right] \\ &= \left[ \frac{d_0}{2\rho} \left[ -i \frac{d^2 f}{dz^2} \right] + i\text{Pe}/2 \left[ 1 + \frac{1}{f^2} \right] \right]. \end{aligned} \quad (3.1)$$

But  $\Phi$  can also be deduced from the solution of the Laplace equation. For the moment, let us write

$$\Phi = \Phi_{\text{Iv}} + (\Phi - \Phi_{\text{Iv}})$$

with

$$\Phi_{\text{Iv}} = \text{Pe}/2 - \text{Pe}(\frac{1}{4} - iz)^{1/2} \quad (3.2)$$

as deduced from (2.5). The correction  $(\Phi - \Phi_{\text{Iv}})$  to the Ivantsov field is given by an integral term derived by Green's-function techniques, as shown in [10], for example. This correction is a small term which is not impor-

tant for the selection process. From (3.1) and (3.2), one obtains

$$-\sigma \frac{d^2 f}{dz^2} + \left[ 1 + \frac{1}{f^2} \right] = (\frac{1}{4} - iz)^{-1/2} + O(\sigma), \quad (3.3)$$

with  $\sigma$  a small parameter, sometimes called the "constant of marginal stability,"  $\sigma = 2d_0/(2\rho\text{Pe}) = 2/C$  (where  $C$  is the usual nonlinear eigenvalue introduced in [10]). The factor 2 is not a pure matter of convenience for the notations. It comes from the chosen model of solidification: here the one-sided model while [10] deal with the symmetric one. Then we easily recover that the constant of stability  $\sigma^*$  for solidification induced by impurities (one-sided model) is twice the value obtained for pure materials (two-sided model). Equation (3.3) is valid only on the interface and  $\sigma$  is an eigenvalue that is determined by the requirement that  $f$  is real at zero ( $\theta$  vanishes at the tip). Let us extend as usual this equation to the complex plane in order to impose a vanishing imaginary part for  $f(\theta)$  on the imaginary axis. But note that here the complex plane is located in the liquid phase. We know from previous treatments that  $\sigma$  is derived from a careful analysis of this nonlinear equation in some inner region where  $f$ , the profile function, becomes singular. This occurs when

$$\frac{1}{f^2} \approx 0 \quad \text{so } (\frac{1}{4} - iz)^{-1/2} \approx 1,$$

which means that this inner region is located on the growth direction, in the liquid phase, at a distance of  $\frac{3}{2}\rho$  from the tip. Let us recall that this singular part of the complex plane, which is in fact located in real space (the liquid) (around point  $I$  in Fig. 1), has a very small extension of order  $\sigma^{2/7}$ . Just to check that this approach is consistent with previous theories, let us analyze this equation and recover that in absence of anisotropy of surface tension, the needle crystal cannot exist due to transcendental small corrections which prevent the tip from being smooth. First of all, we derive the inner equation valid in the boundary layer located at  $P$  [ $x=0, y=\frac{3}{4}(2\rho)$ ] by the following stretching transformation:

$$f = \sigma^{-1/7} F(i\frac{3}{4} + \sigma^{2/7} u). \quad (3.4)$$

To leading orders, from (3.3) it reads

$$-\frac{d^2 F}{du^2} + \frac{1}{F^2} = \frac{1}{2}(iu). \quad (3.5)$$

This is a nonlinear equation which can be solved numerically. But it turns out that we need to know *only* its expansion far away from the inner region, on the growth axis. Everywhere in the complex plane but outside this boundary layer, because  $\sigma$  is a small parameter, one can linearize Eq. (3.3) around the Ivantsov solution  $f_{\text{Iv}}$  given by

$$\frac{1}{f_{\text{Iv}}^2} = (\frac{1}{4} - iz)^{-1/2} - 1.$$

Focusing only on the imaginary part of the small deviation  $(f - f_{\text{Iv}})$  from the Ivantsov solution, hereafter called  $g$  on the imaginary axis ( $z = it$ ), one obtains the

very simple equation

$$\sigma \frac{d^2 g}{dt^2} - 2 \frac{1}{f_{IV}^3} g = 0, \quad (3.6)$$

which is easily solved by WKB techniques:

$$g(t) = AS'(t)^{-1/2} \exp \left[ -\sigma^{-1/2} \int_t^{3/4} du S'(u) \right]$$

with

$$S'(t) = \left[ 2 \frac{1}{f_{IV}^3} \right]^{1/2} = \sqrt{2} [(\frac{1}{4} + t)^{-1/2} - 1]^{3/4}. \quad (3.7)$$

In order to have a smooth solution at the tip without any cusp,  $g(t)$  must vanish at zero, which is possible only if  $A$  equals zero. Since  $A$  is related to the asymptotic expansion of the inner equation, it is really a characteristic of

$$-\sigma(1-\epsilon) \left[ 1 - \frac{\epsilon}{2(1-\epsilon)} \left( f + \frac{1}{f} \right)^4 + \frac{2\epsilon}{1-\epsilon} \left( f + \frac{1}{f} \right)^2 \right] \frac{d^2 f}{dz^2} + \left( 1 + \frac{1}{f^2} \right) = (\frac{1}{4} - iz)^{-1/2} + O(\sigma). \quad (3.9)$$

The same stretching transformation (3.4) transforms (3.9) immediately into

$$-\frac{d^2 F}{du^2} [1 - aF^4] + \frac{1}{F^2} = \frac{1}{2}(iu), \quad a = \frac{\epsilon}{2} \sigma^{-4/7}$$

once we keep only the most singular contribution. Note that  $a$  is a pure number of order unity. This equation has an oscillating behavior near the singular point on the imaginary axis and an exponential decay far away whatever the  $\epsilon$  value. These transcendental decaying corrections can be destroyed by convenient oscillations as well as by convenient values of  $a$ . This is why the anisotropy allows one to recover an infinite discrete set of solutions  $a_n$  such that

$$\sigma = (\epsilon/a_n)^{7/4}.$$

It seems to us that this description of the selection mechanism by surface tension in dendritic growth is much more simple to handle than the usual theories; it also allows one to go a little further by examining the effect of static perturbations. Moreover, it has never been shown that the complex plane of theoreticians is in fact the liquid plane of the experimentalists, at least in dendritic growth. In this sense, one can dream of acting on this complex plane to modify at distances the dendritic growth. The existence of "pure" dendritic growth is explained by the presence of a singularity of the profile function  $f(\theta)$  due to the curvature in some specific place of the liquid phase, on the growth axis, in front of the tip. To act on the growth seems easy: it is enough to create a new singularity in the vicinity of the boundary layer induced by the capillary effects. In the next section we want to emphasize that ordinary localized perturbations which can occur in dendritic growth also make singularities of the temperature field, as well as  $f(\theta)$ , which can compete with the curvature singularity at  $\frac{3}{2}\rho$ .

this inner equation which has no freedom. Numerics indicate that  $A$  is not zero. So there is no needle-crystal solution with isotropic surface tension. The reader can check that we recover the usual transcendental corrections (see, for example, [10]) by a simple change of variable:

$$v = (\frac{1}{4} + t)^{1/2} - \frac{1}{2}.$$

Now we introduce the anisotropy of surface tension in the usual way:

$$\begin{aligned} \gamma(\theta) + \gamma(\theta)'' &= \gamma_0(\theta)[1 - \epsilon \cos(4\theta)] \\ &= \gamma_0(\theta)[1 - \epsilon + 8\epsilon \cos^2\theta - 8\epsilon \cos^4\theta]. \end{aligned} \quad (3.8)$$

Here we assume a fourfold symmetry. With this anisotropic surface tension Eq. (3.3) is modified into

#### IV. LOCALIZED PERTURBATION AS A SINGULARITY OF THE TEMPERATURE FIELD

Any physical effect that moves us away from the ideal situation examined in theories can be called perturbation and it is certain that many of them are present in an ordinary experiment of crystal growth. Moreover, any physicist involved in this field is interested in modifying the selection rule by a quantitative experiment with adjustable amplitude in order to test some aspects of the theories. Most of the time the only parameter at our disposal is the anisotropy of surface tension, which is rather difficult to measure with high precision [4], and most experiments today are concerned with similar samples with similar anisotropies of surface tension. As a consequence, the theory of solvability is hard to test and gives rise to controversy among the community. These controversies are quite inexistent for the Saffman-Taylor viscous fingering, where the equivalent capillary number  $\sigma$  is proportional to the ratio between the surface tension and the velocity of the finger, so it can be modified during the experiment only by pressure. It is a control parameter completely in the hand of the experimentalist, who can observe every finger with arbitrary width  $\lambda > 0.5$ .

First of all, we will distinguish localized perturbations from the long-range ones. The former modify the diffusing field only on distances of order of the natural scale of the dendrite. The latter affect the Ivantsov field everywhere, even at infinity. Although a systematic study has never been done, starting from examples [12,13], we can say that long-range perturbations modify both the relation between the Péclet number and the supersaturation  $\Delta$  (or undercooling) and the nonlinear eigenvalue  $\sigma$ . It is the case, for example, for forced convection in dendritic growth or for coupled diffusion of both impurity and temperature. If one focuses only on the selection mechanism, it turns out that the anisotropy of surface tension, at least for these two cases, which have been studied in some detail [12,13], is the necessary

*ingredient* to obtain selection. Of course, the stability constant deviates from standard predictions with a deviation that depends on the strength of the perturbative field itself. Most of the time, as shown also by experimental results, the deviation of  $\sigma$  appears to be a regular perturbation correction to the value selected by the anisotropy of surface tension and not a singular correction [12,13].

Here we deal with sharply localized perturbations which will not modify the Ivantsov field, like capillary effects. For the moment, we choose them steady in the dendrite frame. They can be inherent of the growth process itself like microscopic germs or nuclei in the bath of the dendrite. They can be due to some inhomogeneity in the experiment or they can be added intentionally by the experimentalist: a rigid obstacle in front of the tip (like coins in the experiment by Thomé *et al.* [7]) or a laser in directional solidification experiments [14]. A simple analysis shows that localized perturbations are responsible for two different kinds of singularity of the field: they produce either a sharp variation of the impurity concentration or a sharp variation of the diffusion coefficient. Sometimes both appear. As an example, a rigid obstacle prohibits the diffusion of impurities inside and imposes the concentration of impurities at the border. Nuclei are equivalent to bubbles in the Saffman-Taylor experiment. They impose the same boundary conditions for the field as for the dendrite: Stefan and Gibbs-Thomson laws. Finally, the laser perturbations locally heat the melt, increasing the diffusion coefficient  $D$  and the miscibility gap. Moreover, the situation here appears more complicated because we cannot neglect the coupling between impurity and temperature in both diffusion equations.

We plan now to represent these perturbations and to calculate the change of the diffusion field  $\phi$  because of these perturbations far away from it. We will show that it produces a dipole perturbation with an amplitude proportional to the involved area, in two dimensions. Let us introduce some effective partial coefficient  $\mathcal{H}$  which relates the equilibrium impurity concentration in the perturbed region  $\mathcal{S}$  to the equilibrium concentration in the liquid, and  $\beta$  the ratio between the diffusion coefficient  $\mathcal{D}$  in the perturbed region  $\mathcal{S}$  and the one of the cell. These two coefficients are enough to describe all these different physical situations.

$$\beta = \mathcal{D}/D \quad \text{and} \quad c_{1\mathcal{S}} = \mathcal{H}c_1 .$$

With these notations, we have  $\phi_{\text{out}} = [c - c_l / (c_l - c_s)] = (c - c_l) / c_l (1 - K)$  outside  $\mathcal{S}$ , but inside  $\mathcal{S}$  it reads

$$\phi_{\text{in}} = \frac{c - \mathcal{H}c_l}{c_l - c_s} = \frac{c - \mathcal{H}c_l}{c_l(1 - K)} ,$$

with  $K$  the usual partition coefficient between the liquid and solid. Now we focus on the boundary conditions to apply at the boundary  $\mathcal{S}$  which, as usual, rest on the conservation of impurity and local equilibrium:

$$\begin{aligned} \phi_{\text{in}} &= \mathcal{H}\phi_{\text{out}} \quad (\text{on the boundary of } \mathcal{S}) , \\ \Psi_{\text{out}}|_{\mathcal{S}} &= \beta\Psi_{\text{in}}|_{\mathcal{S}} + \text{Pe} \frac{1 - \mathcal{H}}{1 - K} x|_{\mathcal{S}} . \end{aligned} \quad (4.1)$$

We choose the usual expansion for the complex potential  $\Phi$  which must satisfy the Laplace equations

$$\begin{aligned} \Phi_{\text{in}} &= \sum_m A_m z^m = \sum_m A_m r^m e^{im\tau} \quad (\text{inside } \mathcal{S}) , \\ \Phi_{\text{out}} &= \Phi_{\text{Iv}} + \sum_m B_m z^{-m} \\ &= \Phi_{\text{Iv}} + \sum_m B_m r^{-m} e^{-im\tau} \quad (\text{outside } \mathcal{S}) , \end{aligned} \quad (4.2)$$

with  $A_m$  and  $B_m$  two sets of complex constants and  $\tau$  the usual polar angle defined from the  $x$  axis. In principle, the above boundary conditions (4.1) are enough to fix the amplitude of each multipole in (4.2). But to simplify the algebra, we will assume that  $\mathcal{S}$  has the shape of a circle of radius  $r_0$  with a center located on the  $y$  axis at the distance  $d$  of the tip. The zeroth-order one is a pure constant irrelevant for selection so we focus on the first one outside the perturbed region. We deduce the amplitude  $\alpha$  of the effective dipole in terms of physical quantities  $r_0$ ,  $\mathcal{H}$ ,  $K$ , and  $\beta$ :

$$B_1 = i\alpha \frac{\text{Pe}}{2} = \frac{i\text{Pe}r_0^2}{2(1 + \beta\mathcal{H})} \left[ \frac{\beta\mathcal{H} - 1}{(\frac{1}{4} + d)^{1/2}} + 2 \frac{1 - \mathcal{H}}{1 - K} \right] . \quad (4.3)$$

The imaginary constant  $i$  means simply that the orientation of the effective dipole is along the growth axis. Note that, when there is no perturbation,  $\beta$  and  $\mathcal{H}$  are equal to unity, and the amplitude of the dipole vanishes. For the coin,  $\beta$  vanishes. Unfortunately we have no general answer about the order of magnitude of  $\mathcal{H}$  compared to  $K$ . It depends on the affinity of the impurities in the liquid for the wall. For the heating by laser, the situation is also not obvious, but if the main effect is the increasing of the diffusion coefficient by the heat,  $\beta$  goes to infinity and  $\alpha$  is also positive. For the case of microscopic germs,  $\beta$  is zero (one-sided model) and  $\mathcal{H}$  is equal to  $K$ , so  $\alpha$  is also positive. It seems to us that most of the localized perturbations reduce to a dipole perturbation with a positive amplitude in the direction of the growth, proportional to  $r_0^2$ , given in units of the radius of curvature of the dendrite.

We cannot use the same technique of analytical functions for the 3D dendritic growth even when axisymmetry is assumed, but, as shown previously, we expect the physics of the growth to be quite independent of the space dimension. The only technique at our disposal in this case remains the Green's-function technique with introduction of the perturbation. In order to carry out a numerical analysis of the deduced equation, it is rather important to show that also in 3D most of the perturbations are equivalent to a dipole parallel to the growth axis, and to evaluate its amplitude in order to see if it has some chance to act on the growth. First of all, from Ivantsov theory, we can deduce the temperature field in the zero Péclet number limit:

$$\phi_{\text{Iv}} = -\frac{\text{Pe}}{4} \ln 2 \left[ \left( z + \frac{1}{4} \right) + R \right]$$

$$\text{with } R = [(\rho^2 + (z + \frac{1}{4})^2)^{1/2}]$$

[ $z$  and  $\rho$  define the polar coordinates,  $\rho = (x^2 + y^2)^{1/2}$ ].

The general solution of the Laplace equation for the 3D axisymmetric case is

$$\phi = \phi_{\text{Iv}} + \sum_l \left[ \left[ A_l r^l + \frac{B_l}{r^{l+1}} \right] P_l(\cos\theta) \right].$$

Only the second equation in Eq. (4.2) has to be modified since we cannot define easily a stream function  $\Psi$ . It is transformed into

$$\mathbf{n} \cdot \nabla \phi_{\text{out}} = \beta \mathbf{n} \cdot \nabla \phi_{\text{in}} - \text{Pe} \cos(\theta) \frac{1 - \mathcal{H}}{1 - K}. \quad (4.4)$$

Solving the first equation (4.2) and Eq. (4.4), we find an amplitude very similar to (4.3):

$$B_1 = \alpha \frac{\text{Pe}}{2} = \frac{\text{Pe} r_0^3}{2(2 + \beta \mathcal{H})} \left[ \frac{\beta \mathcal{H} - 1}{2(d + \frac{1}{4})} + 2 \frac{1 - \mathcal{H}}{1 - K} \right]. \quad (4.5)$$

The formula (4.5) is rather close to the one calculated in 2D (4.3) despite some numerical factors. Nevertheless, the amplitude of this dipole will be rather different since, in 3D, it is proportional to the perturbed volume ( $r_0^3$ ), contrary to the 2D case ( $r_0^2$ ). We will come back to this difference in Sec. VI, where numerical results are discussed. The discussion concerning the sign of this 3D dipole is the same as in 2D: most of the time, it is positive.

One can wonder if it is realistic to consider a static perturbation in the dendrite frame since most of the perturbations are static in the laboratory frame. We can argue that when the perturbation is due to some fluctuation it is not a rigid one; it can be advected by the flow created by the dendrite, so this perturbation will be perfectly static in the dendritic frame. On the contrary, a rigid obstacle in the laboratory frame moves in the dendrite frame with a characteristic time of order  $\tau_0 = \rho/U$ . This time is much greater than the characteristic time of sidebranching given by  $\tau_s = \sigma^{1/2} \tau_0$ , which is itself much greater than the diffusion time  $\tau_D = \text{Pe} \tau_0$  (for a discussion of these time scales see, for example, [16]). So the time of displacement  $\tau_0$  in the dendrite frame is very large and the perturbation can be considered as static in the dendrite frame, except perhaps in the very close vicinity of the tip. The dendrite has time enough to adjust its tip radius to each instantaneous position of the dipole. We will use this adiabatic approximation and will assume that the dipole is steady in the frame of the needle crystal.

## V. SELECTION IN THE PRESENCE OF STATIC LOCALIZED PERTURBATION: ANALYTIC TREATMENT

This section is devoted to the determination of the eigenvalue  $\sigma$  in the presence of a dipolar perturbation. In order to show the drastic effect of a localized perturbation located in the vicinity of the growing structure, we will examine the ideal case where there is no needle-crystal solution: that is, we will assume that the surface tension is isotropic. Since most of the localized perturbations are of dipolar nature, we will restrict ourselves to this kind of dipolar interaction. Moreover, we have

shown that the orientation of the dipole is parallel to the growth axis, its position is fixed at a distance  $d$  from the tip on this axis, and its amplitude is characterized by a parameter  $\alpha$ , which happens to be positive in physical situations. The complex potential which acts everywhere in the cell is the sum of the Ivantsov potential plus the dipolar potential,

$$\Phi = \Phi_{\text{Iv}} + \frac{\alpha \text{Pe}}{2} \frac{i}{z - id}. \quad (5.1)$$

Because of this perturbation, we need to add the complex derivative of the dipolar potential to the interface relation (3.3), assumed to be valid everywhere in the liquid.

$$-\sigma \frac{d^2 f}{dz^2} + \left( 1 + \frac{1}{f^2} \right) = \left( \frac{1}{4} - iz \right)^{-1/2} - \alpha \frac{1}{(z - id)^2} + O(\sigma). \quad (5.2)$$

Singularities of this equation correspond to  $1/f \rightarrow 0$ . There will be three singularities, but if we choose  $\alpha$  small, one of them remains close to the previous one:  $z = 3i/4$ , the others being located near  $id$ . In the following, we will restrict ourselves to this situation:  $\alpha$  small, in order to simplify the analysis. Of course, when  $d$  is close to  $\frac{3}{4}$ , all of the singularities are in the same neighborhood. As before, the solvability condition requires that the imaginary part of  $f$  vanishes on the imaginary axis far away from each singularity. So we introduce the change of variable  $z = it$ .

$$\sigma \frac{d^2 f}{dt^2} + \frac{1}{f^2} = \alpha \frac{1}{(t - d)^2} - g(t) + O(\sigma)$$

with  $(5.3)$

$$g(t) = 1 - \left( \frac{1}{4} + t \right)^{-1/2}.$$

We focus on the boundary layer around  $t = d$  and we linearize  $g$ . Moreover, we apply a stretching transformation:

$$u = [g'(d)/\alpha]^{1/3} (t - d), \quad F = fg'(d)^{1/3} \alpha^{1/6}, \quad (5.4)$$

$$\eta \frac{d^2 F}{du^2} + \frac{1}{F^2} = \frac{1 + \beta u^2 - u^3}{u^2},$$

with

$$\eta = \frac{\sigma}{\alpha^{7/6} g'(d)^{1/3}}, \quad \beta = - \frac{g(d)}{\alpha^{1/3} g'(d)^{2/3}}. \quad (5.5)$$

Note that  $g'(d)$  is always positive but  $g(d)$  is either positive for  $d > \frac{3}{4}$  or negative for  $d < \frac{3}{4}$ . The selection mechanism now means one relation between  $\eta$  and  $\beta$ . Equation (5.4) is exactly the Combescot-Dombre inner equation [8] for the coupled selection problem of a bubble in front of a finger in the Hele-Shaw cell. Anyway, some differences appear: because they have to select both the bubble and the finger sizes for fixed  $d$ , both parameters  $\eta$  and  $\beta$  need to be selected and are positive eigenvalues of order unity. It means that, in our language, the amplitude of the equivalent dipole which is related to the bubble size is fixed in their case. In our case, the amplitude of the dipole is a free parameter so the selection produces

richer pictures of scaling laws, which depend on the two characteristic parameters of the dipole: the amplitude and position.

The capillary effects plus the dipole effects induce a regular correction to the Ivantsov parabola if the imaginary part of  $F$  vanishes far away from the singularities. This is possible, as shown in detail in [8], if and only if the cubic polynome on the right-hand side of Eq. (5.4) has two complex-conjugate roots. It immediately produces a lower limit to our parameter  $\beta > \beta_c = -(27/4)^{1/3}$ . It means that  $d$  should be smaller than  $d_{cr}$ , given by

$$d < d_{cr} \quad \text{with} \quad d_{cr} = \frac{3}{4} + \left(\frac{27}{2}\alpha\right)^{1/3} \quad (5.6)$$

for small  $\alpha$  values.

Now, two cases have to be handled following the order of magnitude of  $\eta$  compared to 1.

(a) When the parameter  $\eta$  is small, the selection gives us the following relation:

$$d_{cr} - d = (b_n \eta)^{2/5} \alpha^{1/3}. \quad (5.7)$$

$b_n$  represents an increasing set of nonlinear eigenvalues.

(b) The opposite limiting case is concerned with large values of  $\eta$ , and so  $\beta$ , which means  $\sigma > \alpha^{7/6}$ . The analysis is more complex since two opposite situations can appear.

(i) The first possibility, which is the most natural one, is to neglect the cubic term in the polynome of Eq. (5.4), and thereby restrict the inner problem to the dipole singularity. This also implies that one modify the stretching of Eq. (5.4). If both  $u$  and  $F$  are scaled by  $\beta^{-1/2}$ , we find that  $\eta$  should scale like  $\beta^{1/2}$  so that

$$u = v \beta^{-1/2}, \quad F = G \beta^{-1/2}.$$

If we define  $c = \beta^{1/2}/\eta$ , it gives the following inner equation:

$$c^{-1} \frac{d^2 G}{dv^2} + \frac{1}{G^2} = \frac{1+v^2}{v^2} \quad (5.8)$$

and the following selection rule for  $\sigma$ :

$$c_n \sigma = \alpha |g(d)|^{1/2}. \quad (5.9)$$

As usual, the largest value of  $\sigma$  in the spectrum (5.9) corresponds to an eigenvalue  $a$  of order unity, and lower values of  $\sigma$  correspond to larger eigenvalues  $c_n$  which become proportional to  $n^2$  when  $n$  is large. (ii) The second possibility involves the case  $\eta \gg \beta^{1/2}$ . Of course, it is impossible to find this kind of solution in the framework of Eq. (5.8) which rests on the opposite scalings. Note that, because of the definitions given by (5.5), this hypothesis implies larger values of  $\sigma$  when compared to (5.9). This situation is important since usually experimental measurements are concerned with the largest value of  $\sigma$ . All the other selected steady states appear to be instable and so are not observed. It is easier to come back to our original equation (5.3). In this case, which corresponds to  $\alpha$  extremely small, both singular regions (one around  $d$ , the other around  $\frac{3}{4}$ ) are well separated. So the imaginary contribution coming from the most distant singularity from the tip (that is, the usual one), although weakened

by a decreasing exponential factor, succeeds to combine with the very weak dipole contribution (proportional to  $\alpha$ ).

Taking into account the decreasing contribution from (3.7), it reads

$$\exp \left[ -\sigma^{-1/2} \int_d^{3/4} du S'(u) \right] \approx \alpha. \quad (5.10)$$

So, within logarithmic accuracy, we neglect the Van Vleck prefactor which involves only powers of  $\sigma$  in (5.9). It reads

$$\sigma = \frac{[S(\frac{3}{4}) - S(d)]}{(\ln \alpha)^2}. \quad (5.11)$$

We want to emphasize that when the parameter  $\alpha$  responsible for the selection goes to zero, the selected eigenvalue  $\sigma$  goes to zero in different ways for the main branch (5.11) and the other branches given by (5.9). This is clearly a new result since usual eigenvalues  $\sigma_n$ , selected by anisotropy of surface tension, differ only by numerical factors.

Let us sum up. First we eliminate the case (b ii), which corresponds to extremely small values of the amplitude of the dipole  $\alpha$  (with  $|\ln \alpha|$  large). Two opposite situations can occur following the distance of the dipole from the curvature singularity compared to  $\alpha^{1/3}$ . If this distance  $|d - \frac{3}{4}|$  is small,  $|d - \frac{3}{4}| < \alpha^{1/3}$ , then  $\sigma$ , given by (5.7), is proportional to  $\alpha^{4/3}$ . In the opposite situation,  $|d - \frac{3}{4}| > \alpha^{1/3}$ ,  $\sigma$  is proportional to  $\alpha$  as shown by (5.9). Between these two limits,  $\eta \ll 1$  described by (5.7) and  $\eta \gg 1$  described by (5.8) or (5.11), there is an intermediate regime where  $\eta$  and  $\beta$  in (5.5) are of order unity. This intermediate regime can be handled numerically and is the subject of the next section. But in any case, we have shown that a localized dipolar perturbation can also be responsible of the fixed point of the needle-crystal growth since our analysis is concerned with isotropic surface tension. Of course, this fixed point depends on both the amplitude and the position of the dipole. It seems that these dipoles, which are probably always present in an experiment, are in competition with the anisotropy of surface tension, which is generally believed to be responsible for selection. It will be rather tedious to analytically handle this competition. This is why we now present a numerical analysis with realistic values of both the dipole amplitude and the anisotropy. We should emphasize that the selection by dipolar perturbation takes place only for a precise sign of the dipole. For the opposite sign, we did not find a solution to the selection problem both analytically and numerically, but most of the perturbations examined in this section seem to correspond to this situation with selection.

## VI. NUMERICAL INVESTIGATION OF THE 2D AND 3D NEEDLE CRYSTAL IN THE PRESENCE OF DIPOLE PERTURBATION

Numerics allow one to handle intermediate values of the parameters which are very often closer to the experimental ones than the asymptotic regime treated in the previous section. Moreover, it will allow a discussion

about the physical relevance of this treatment. We use our code of the needle-crystal growth in 2D and 3D cases (with axisymmetry) [10,16] at zero Péclet number and in the two-sided model of solidification. Results concerning  $\sigma$  are expected to be different only by a numerical factor of 2 since the framework of the analytical part is the one-sided one. This code rests on a solution of the interface equation derived by Green's-function technique. We add the dipole perturbation of amplitude  $\alpha$  located on the growth direction at a distance  $d$  from the tip. First of all, we verify different aspects of the analytical results explained above in absence of anisotropy of surface tension. Second, we include ordinary anisotropy values ( $\epsilon=0.083$  for succinonitrile,  $\epsilon=0.375$  for pivalic acid).

#### Isotropic needle-crystal growth with dipole interaction

The previous analytical treatment handles dimensionless quantities such as the dipole amplitude  $\alpha$  or its position  $d$  scaled by the unknown radius of curvature of the selected dendrite. These units are appropriate for the analytical treatment but not for experimental comparisons. In that sense, it is not really easy to predict the final result in a given experiment from the analytical part above. Anyway, since the analytical treatment announces a rather important result, that is, selection by dipole perturbation with isotropic surface tension, it seems to us rather important to verify carefully some scaling laws. In a second step, we will focus on the physical relevance for the experiments. A first check consists in the scaling law of Eq. (5.7). Figure 2 displays the selected values of  $\sigma^*$ , the usual constant of stability measured by the experimentalists, versus the dimensionless position of the dipole  $d$ , for fixed  $\alpha=10^{-3}$ . In the case of solidification induced by diffusion of impurity,  $\sigma^*$  is eight times greater than our parameter  $\sigma$  introduced previously. Our numerical  $\sigma^*$  values confirm that  $\sigma^*$  goes to 0 when  $d$  goes to  $d_{cr} \approx \frac{3}{4}$ , proving that there is no steady state for the needle crystal when the dipole is too far from the tip, in agreement with the prediction of (5.6) and (5.7)

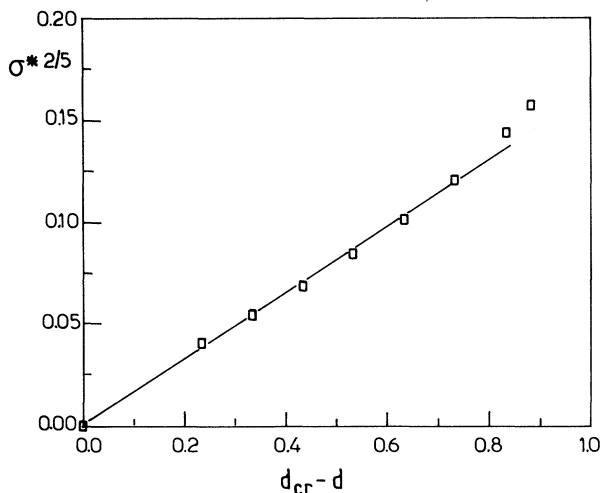


FIG. 2. The selected  $\sigma^*$  values vs the position of the dipole when its amplitude is  $\alpha=0.001$ . Following Eq. (4.6)  $d_{cr}=0.938$ .

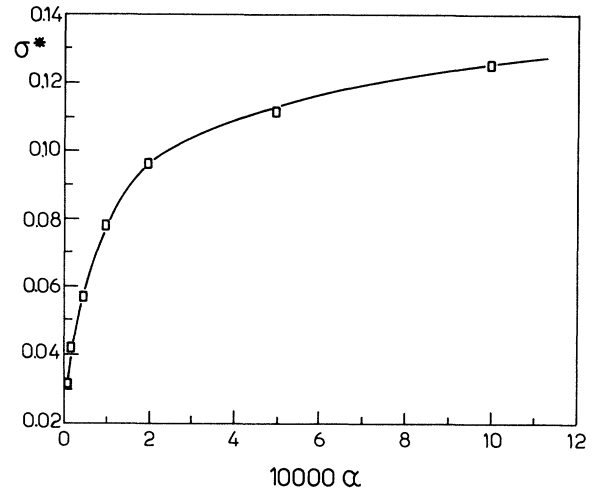


FIG. 3. Selected values of  $\sigma^*$  vs the amplitude  $\alpha$  of the dipole  $a$  when the position  $d=0.1$  is rather different from  $d_{cr}$ . Note that  $\sigma^*$  is very similar to measured values in dendritic-growth experiments.

and also in agreement with our physical intuition. It also emphasizes the specific role played by the point  $\frac{3}{2}\rho$  in front of the tip, similar to what is observed for the viscous fingering experiment. As an illustration we present also the dependence of  $\sigma$  vs  $\alpha$  for fixed  $d$  in an intermediate regime, when  $d=0.1$  is rather far away from  $d_{cr}$  (Fig. 3). Finally we made successful trials to verify the logarithmic scaling (5.11), which is possible due to the very slow decaying of  $\sigma$  vs  $\alpha$  when  $\sigma \rightarrow 0$ , as shown by Fig. 4. This logarithmic scaling is pertinent only for extremely low values of the parameter  $\alpha$ .

Let us come back now to universal units more practical for the experiments. We are looking for the unknown radius of curvature of the selected dendrite by dipolar perturbation. We scale all lengths (that is, the radius of cur-

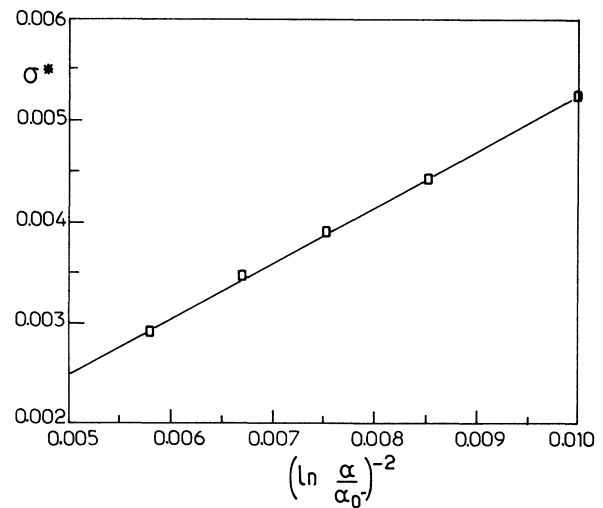


FIG. 4. Logarithmic scaling of  $\sigma$  vs the amplitude  $\alpha$  of the dipole following Eq. (4.2).  $\alpha_0$  has been found by trials.



vature and the dipole position) by  $d_0/\text{Pe}$ , where  $d_0$  is the capillary length and  $\text{Pe}$  is fixed by the supersaturation following Ivantsov's relation. As a consequence the amplitude of the dipole, in physical units, is given by

$$\alpha' = \frac{r_0^D \text{Pe}^D}{d_0^D}, \quad (6.1)$$

where  $D$  is the space dimension. This last formula allows a realistic evaluation: let us assume that the size of the perturbed area is ten times smaller than the typical length of a dendrite, that is,  $1 \mu\text{m}$ ; the  $\text{Pe}$  number in 2D is rather small, of order  $10^{-2}$ , proportional to  $\Delta^2$  (this number is a little larger in 3D, roughly proportional to  $\Delta$  [9]); and the capillary length is of order  $10\text{--}100 \text{ \AA}$ . A realistic dimensionless value of the dipole amplitude seems to be of order several hundred in 2D, depending on the experiment, and in 3D one or two orders of magnitude greater. In Fig. 5 (Fig. 6) we plot the selected radius of curvature in 2D (3D) versus the distance  $d$  from the tip of the dipole. Note that the selected value has the same order of magnitude as usually observed in dendritic growth. In these units,

$$\rho_{\text{sym}} = \frac{4}{\sigma_{\text{sym}}^*} \frac{d_0}{\text{Pe}}.$$

With, for example,  $\sigma \approx 0.011$  for succinonitrile material, this gives

$$\rho_{\text{sym}} \approx 400.$$

For the one-sided solutal dendritic growth, the radius of curvature is divided by 2.

As shown by Figs. 5 and 6, in the range of accessible numerical values, it turns out that this radius is proportional to the distance that separates the dipole from the tip at fixed amplitude. The dendrite becomes more and more sharp-pointed when the amplitude of the perturba-

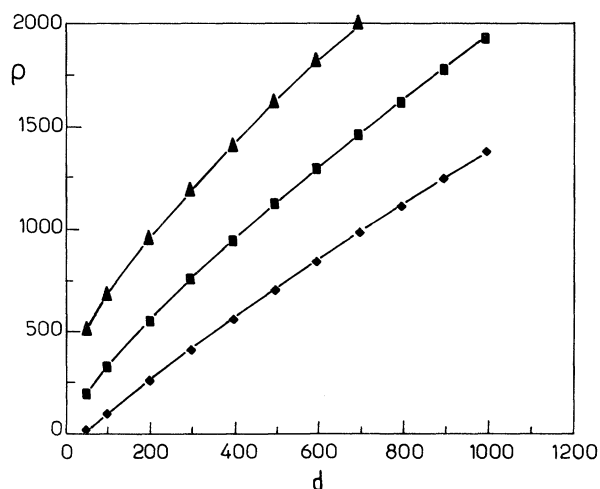


FIG. 5. Radius of curvature  $\rho$  of the 2D needle crystal selected by dipolar perturbation vs the position  $d$  of the dipole. The two-sided model of solidification is assumed. The unit of length is  $d_0/\text{Pe}$ .  $\blacktriangle$ ,  $\alpha' = 2$ ;  $\blacksquare$ ,  $\alpha' = 20$ ;  $\blacklozenge$ ,  $\alpha' = 200$ .

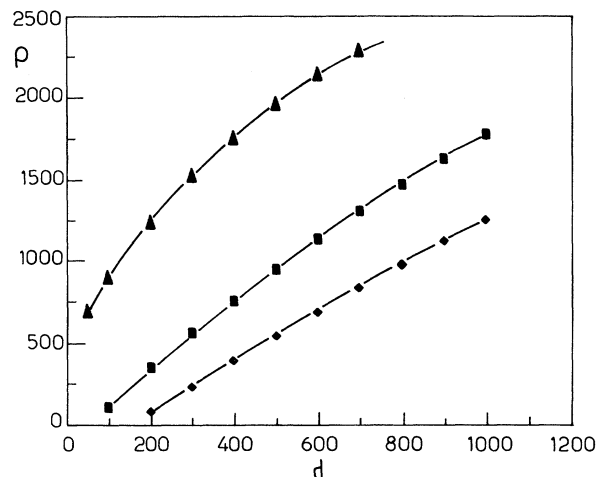


FIG. 6. Radius of curvature  $\rho$  of the 3D needle crystal selected by dipolar perturbation vs the position  $d$  of the dipole. The two-sided model of solidification is assumed. The unit of length is  $d_0/\text{Pe}$ .  $\blacktriangle$ ,  $\alpha' = 200$ ;  $\blacksquare$ ,  $\alpha' = 20\,000$ ;  $\blacklozenge$ ,  $\alpha' = 200\,000$ .

tion is increased and also when the position of the dipole is closer to the tip. Finally, one can notice that this result is somewhat different from the conclusion derived in the Saffman-Taylor case. In viscous fingering with a bubble, Thomé, Combescot, and Couder [7] concluded that the final selected  $\lambda$  relative width of the finger is such that there is a complete collapse between singularities of the Saffman-Taylor velocity field and the dipole position. This collapse allows a very easy determination of  $\lambda$  which is independent of the amplitude of the fictitious dipole and also of the size of the bubble. This was in agreement with the experimental measurements. If one keeps this very nice and simple picture, in our language it will mean that the radius of curvature of the dendrite is simply  $\frac{2}{3}d$ , whatever the value of the dipole amplitude. Figures 5 and 6 prove without any ambiguity that this is not the case since a sharp dependence with amplitude is observed. So the dendritic growth appears to be a more complicated example for testing a singularity in real space. Nevertheless, our results show the importance of static and localized perturbations in crystal growth as far as selection mechanism is involved.

Let us discuss now the selection with both anisotropy of surface tension and dipole perturbation. Since both effects can be responsible for selection, there is a nontrivial competition between them which makes the final result difficult to predict. Nevertheless, when the dipole is far away from the tip, we expect the selection to be produced by the anisotropy of surface tension which fixes the radius of curvature of the dendrite  $\rho_{\text{anis}}$ . When the distance of the dipole from the tip becomes of order of this value  $\rho_{\text{anis}}$ , selected values of  $\sigma$  and  $\rho$  will be changed. We expect that for the "good sign" of the dipole which has always been considered in this paper (which means  $\alpha$  positive in our terms), the dendrite would be sharper, so  $\rho$  would decrease with an increase of  $\sigma$  and growth velocity. These qualitative predictions are confirmed by numerics as shown in Figs. 7 (for 2D) and 8 (for 3D),

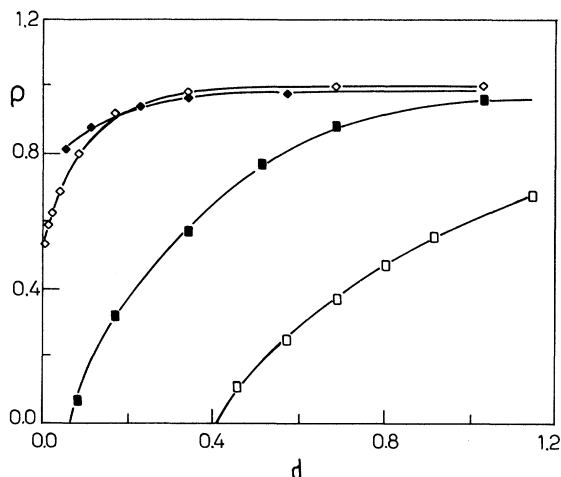


FIG. 7. Radius of curvature  $\rho$  of the 2D needle-crystal selected by dipolar perturbation vs the position  $d$  of the dipole for two different values of anisotropy of surface tension  $\epsilon=0.083$ ,  $\epsilon=0.375$ . The two-sided model of solidification is assumed. The unit of length is the value of  $\rho$  selected by anisotropy with  $\sigma_{an}^*=0.014$  for  $\epsilon=0.083$  and  $\sigma_{an}^*=0.091$  for  $\epsilon=0.375$ . For  $\epsilon=0.083$ ,  $\blacklozenge$ ,  $\alpha'=2$ ,  $\blacksquare$ ,  $\alpha'=200$ . For  $\epsilon=0.375$ ,  $\diamond$ ,  $\alpha'=2$ ;  $\square$ ,  $\alpha'=200$ .

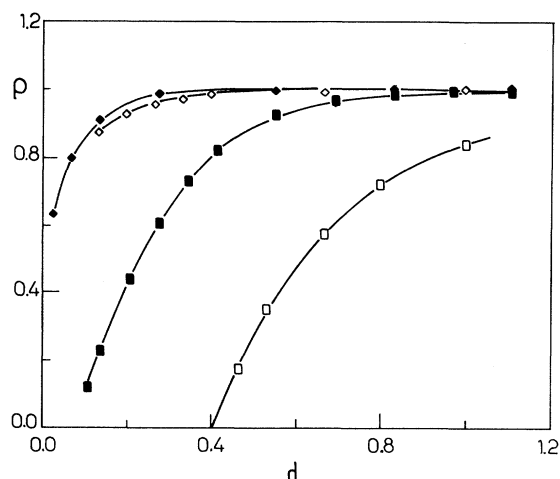


FIG. 8. Radius of curvature  $\rho$  of the 3D needle crystal selected by dipolar perturbation vs the position  $d$  of the dipole for two different values of anisotropy of surface tension  $\epsilon=0.083$ ,  $\epsilon=0.375$ . The two sided model of solidification is assumed. The unit of length is the value of  $\rho$  selected by anisotropy with  $\sigma_{an}^*=0.011$  for  $\epsilon=0.083$ , and  $\sigma_{an}^*=0.053$  for  $\epsilon=0.375$ . For  $\epsilon=0.083$ ,  $\blacklozenge$ ,  $\alpha'=200$ ;  $\blacksquare$ ,  $\alpha'=20\,000$ . For  $\epsilon=0.375$ ,  $\diamond$ ,  $\alpha'=200$ ;  $\square$ ,  $\alpha'=20\,000$ .

where the calculations assume the anisotropy value of succinonitrile ( $\epsilon=0.083$ ) and of pivalic acid ( $\epsilon=0.375$ ). The reader can expect that, for smaller values of anisotropy, the effect of dipolar perturbation will be stronger. On the contrary, for larger values of anisotropy, such as for pivalic acid, the dipolar perturbations would be ineffective except in the very close vicinity of the tip. This is not true, as shown by Figs. 7 and 8. When the dipolar perturbation is weak, its influence on  $\sigma^*$  is weak, of course, and quite independent of the anisotropy values. On the contrary, when it increases, anisotropic materials appear to be more sensitive. This astonishing result is due to the fact that the efficient amplitude of the dipole increases when the "natural" tip radius of the dendrite decreases and when the anisotropy of surface tension increases. Note that these conclusions will be reversed in the case where the sign of the dipole will be changed too. This can happen by a physical effect not involved here. We can conclude that most of the axial perturbations will be responsible for a too large measurement of the constant of stability  $\sigma^*$ , when compared to values deduced from anisotropy of surface tension.

## VII. CONCLUSION

We have found a selection mechanism of the dendritic growth by localized perturbations of the diffusive field which can be controlled experimentally. It can explain the existence of needle crystals without assuming anisotropy of surface tension. This paper shows the extreme sensitivity of the selection process against physical per-

turbations always present in laboratory experiments. It also stresses the difficulty of testing the solvability mechanism by anisotropy of surface tension. Due to this difficulty, contradictory points of view appear in the literature. The main difficulty remains the precise determination of the properties of the concerned materials. It is why an attempt has been made for precise measurements of the anisotropy of surface tension for succinonitrile and pivalic acid [4]. Nevertheless, a certain discrepancy remains, which is probably due to the difficulty of treating in the theoretical treatment all perturbations which cannot be avoided in a real experiment. We simply show here that a static dipole in the dendrite frame can be responsible of the factor of 2 or 3 which separate measurements from theoretical predictions. This is only a model which shows the extreme sensitivity of the selection mechanism. This paper confirms that it is possible to act on fronts of solidification, at distances and without touching it.

## ACKNOWLEDGMENTS

It is a pleasure to acknowledge very helpful and enlightening discussions with R. Combescot, H. Cummins, Y. Couder, and V. Hakim. This work was supported in part by the "A.T.P.: CNES-CNRS." E. Brener has been supported by the Ministère de la Recherche et de la Technologie. Laboratoire de Physique Statistique is "associé au C.N.R.S. et aux Universités Paris VI et Paris VII."

- \* Permanent address: Institute for Solid State Physics, Chernogolovka, Russia.
- [1] G. P. Ivantsov, *Dok. Akad. Nauk SSSR* **58**, 567 (1947).
- [2] J. S. Langer, *Rev. Mod. Phys.* **52**, 1 (1980), in *Lectures in the Theory of Pattern Formation*, Les Houches Vol. XLVI (Elsevier Science, New York, 1986); D. A. Kessler, J. Koplik, and H. Levine, *Adv. Phys.* **37**, 255 (1988); E. A. Brener and V. I. Melnikov, *ibid.* **40**, 53 (1991); Y. Pomeau and M. Ben Amar, in *Solids Far from Equilibrium*, edited by C. Godreche (Cambridge University Press, Cambridge, England, 1992).
- [3] M. Ben Amar and Y. Pomeau, *Europhys. Lett.* **2**, 307 (1986); A. Barbieri, D. C. Hong, and J. S. Langer, *Phys. Rev. A* **35**, 1802 (1987).
- [4] M. E. Glicksman, R. J. Schaefer, and J. D. Ayers, *Metall. Trans. A* **7**, 1747 (1976); S. C. Huang and M. E. Glicksman, *Acta Metall.* **29**, 701 (1981); **29**, 717 (1981); J. P. Gollub, in *Growth and Forms, Non-linear Aspects*, edited by M. Ben Amar, P. Pelcé, and P. Tabeling (Plenum, New York, 1988); M. Muschol, D. Liu, and H. Z. Cummins, (unpublished).
- [5] M. Ben Amar, *Phys. Rev. A* **44**, 3673 (1991).
- [6] P. G. Saffman and G. Taylor, *Proc. R. Soc. London Ser. A* **245**, 313 (1958); J. W. McLean and P. G. Saffman, *J. Fluid Mech.* **102**, 455 (1981).
- [7] H. Thomé, R. Combescot, and Y. Couder, *Phys. Rev. A* **41**, 5739 (1990).
- [8] R. Combescot and T. Dombre, *Phys. Rev. A* **39**, 3525 (1989).
- [9] P. Pelcé, *Dynamics of Curved Front* (Academic, New York, 1988).
- [10] P. Pelcé and Y. Pomeau, *Stud. Appl. Math.* **74** 245 (1986); M. Ben Amar and B. Moussallam, *Physica D* **25**, 155 (1987).
- [11] R. Feynman, R. Leighton, and M. Sands, *Feynman Lectures on Physics* (Addison-Wesley, Reading, MA, 1964), Vol. II. Chap. 7-4.
- [12] A. Karma and J. S. Langer, *Phys. Rev. A* **30**, 3147 (1984); M. Ben Amar and P. Pelcé, *ibid.* **39**, 4263 (1989).
- [13] M. Ben Amar and Y. Pomeau, *PCH* **11**, 617 (1989); P. Bouissou and P. Pelcé, *Phys. Rev. A* **40**, 6673 (1989).
- [14] X. W. Qian and H. Z. Cummins, *Phys. Rev. Lett.* **64**, 3038 (1990).
- [15] M. Barber, A. Barbieri, and J. Langer, *Phys. Rev. A* **36**, 3340 (1987).
- [16] M. Ben Amar, *Phys. Rev. A* **41**, 2080 (1990).